CHAPTER EIGHTEEN

Split T7 RNA polymerase biosensors to study multiprotein interaction dynamics

Jeffrey A. Dewey, Bryan C. Dickinson*
Department of Chemistry, The University of Chicago, Chicago, IL, United States
*Corresponding author: e-mail address: dickinson@uchicago.edu

Contents

Abstract

Protein-protein interactions (PPIs) are involved in nearly all cellular processes. PPIs are particularly crucial for mediating selectivity along signaling pathways. Thus, measuring the competitive interplay between PPIs in a cell is important for both understanding fundamental cellular regulation and developing therapeutics targeting those whose dysregulation is associated with disease. A variety of split protein reporter-based tools are available to measure if two proteins interact within a cell and thereby characterize the general determinants of their interactions. PPIs, however, occur within complex networks facilitated by dynamic biophysical nuances that determine activity and selectivity. Evolved, proximity-dependent split T7 RNA polymerase (RNAP) biosensors have recently been used to perform deep mutational scanning of PPI interfaces, and to create synthetic gene circuits. In this chapter, we present the application of proximity-dependent split RNAP biosensors as a method to measure multidimensional PPIs in live cells. Orthogonal split RNAP "tags" encode each interaction in a unique RNA signal, thereby enabling the study of multiple competitive PPIs in live cells. Each unique RNA signal can be quantified via established RNA analysis methods. Herein, we provide advice and

Methods in Enzymology, Volume 641
ISSN 0076-6879
https://doi.org/10.1016/bs.mie.2020.04.047

© 2020 Elsevier Inc.
All rights reserved.

protocols to aid other researchers in using the split RNAP biosensor, focusing primarily on how to detect multiple PPIs in mammalian cells, including their dynamic interplay in the presence of small molecule inhibitors.

1. Introduction

Protein-protein interactions (PPIs) are involved in nearly all cellular processes, particularly in higher organisms. For example, although there are only approximately 21,000 protein coding genes in the human genome there are an estimated 650,000 unique PPIs, ranging from simple binary interactions to multiprotein complexes (Stumpf et al., 2008). These interactions regulate information flow through the central dogma, cell signaling, metabolic processes, and more (Eliseev et al., 2018; Kim et al., 2018; Plaschka et al., 2016). As the PPI estimation implies, individual proteins can take part in any number of distinct PPIs, with each one potentially involved in a different cellular process. Therefore, traditional methods for studying protein function, e.g., protein overexpression and knockdown, can impact several pathways simultaneously, convoluting experimental results. There are numerous instances where genetic aberrations cause human disease via PPI dysregulation or can be alleviated by manipulating selective PPIs (Soucek et al., 2013; Souers et al., 2013). This central role of PPIs has led researchers to develop tools to study natural PPIs, and even to manipulate biology via synthetic PPI signaling (Langan et al., 2019).

A variety of methods have been developed to study PPIs, ranging from fixed-cell antibody-based endogenous coimmunohistology to live-cell FRET-based kinase sensors (Fig. 1) (Sun, Hays, Periasamy, Davidson, & Day, 2012; van der Geer, 2014). In this chapter, we will focus on measuring PPIs in live cells. In the context of live-cell PPI detection, protein fragment complementation (PFC) is one of the most widely used and powerful approaches (Jones, Zinkus-Boltz, & Dickinson, 2019). PFC assays work by splitting a reporter protein (GFP, luciferase, etc.) and genetically tagging each split protein fragment to different proteins of interest. Only when the tagged proteins come within close proximity to one another does the split reporter reassemble to produce an output signal. Indeed, this approach has been widely used with light-emitting reporters, including GFP and luciferase, to study and discover chemical inhibitors of PPIs (Hall et al., 2012;

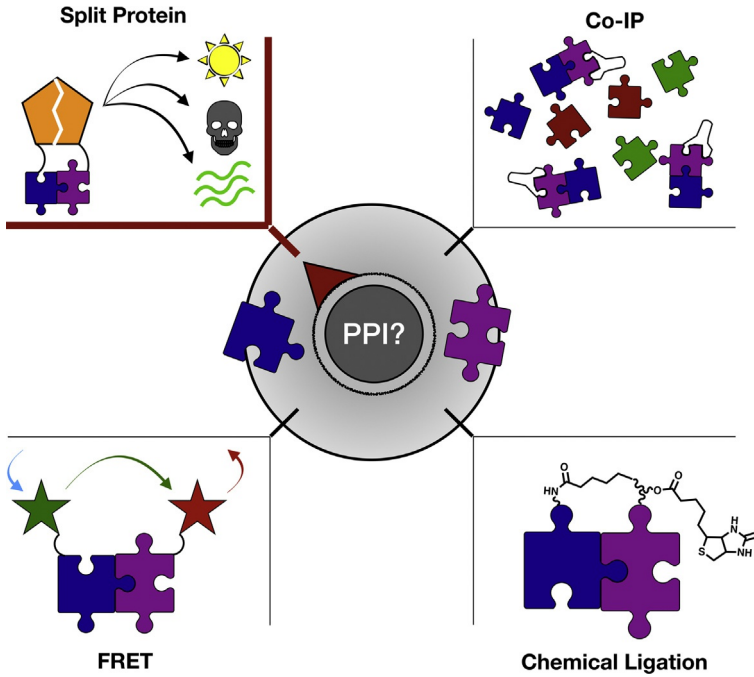

Fig. 1 Schematic of several common methods for detecting PPIs. This chapter focuses on the split T7 RNAP, and so split proteins, which can produce diverse signals such as light, cytotoxic small molecules, or RNA, are highlighted.

Hu & Kerppola, 2003; Ozawa, Kaihara, Sato, Tachihara, & Umezawa, 2001; Wehr & Rossner, 2016). More recently developed PFCs such as split horseradish peroxidase and split BS2 esterase convert PPIs into activation of chemical probes that release light, kill surrounding cells, or label surrounding proteins with chemical tags (Jones, Kentala, et al., 2019; Jones, Zinkus-Boltz, et al., 2019; Martell et al., 2016). While these aforementioned PFC tools are powerful for measuring a single PPI, they are often unable to measure or discern signals from multiple simultaneous interactions, largely due to a lack of orthogonal split components, or spectral overlap in output signals. Split RNAP-based biosensors, however, benefit from the vast information storage capacity of RNA to in principle encode an array of molecular interactions for subsequent multiplexed analysis. This chapter will therefore describe the evolved split T7 RNA polymerase (RNAP), a novel PFC capable of converting multiple PPIs into unique RNA outputs simultaneously in live cells.

2. Evolution of the split T7 RNA polymerase biosensor

2.1 Split T7 RNAP biosensor history and nomenclature

In 1985 (Tabor & Richardson, 1985) it was discovered that the T7 RNAP, a single-domain, highly active, RNAP retained its transcriptional activity upon proteolysis into two fragments. Much later, Shis et al. confirmed the two fragments could reassemble when coexpressed (Shis & Bennett, 2013). In 2014 Segall-Shapiro et al. discovered that there are in fact multiple locations in T7 RNAP that are amenable to splitting and reassembly to produce a fully functional RNAP (Segall-Shapiro, Meyer, Ellington, Sontag, & Voigt, 2014). One split site at amino acid position 181 produced particularly robust signal when the N-terminal half of the RNAP (aa's 1-180; wtRNAP$_N$) was coexpressed with the C-terminal half of the RNAP (aa's 181-883; RNAP$_C$), which contains the protein domain that recognizes the DNA promoter sequence. This group went on to introduce known amino acid mutations into this promoter recognition domain, generating a series of unique RNAP$_C$'s that recognize orthogonal DNA promoters. For example, the wild type RNAP$_C$ recognizes the T7 DNA promoter, and is termed the T7-RNAP$_C$, but an RNAP$_C$ mutant only recognizes the orthogonal CGG DNA promoter (CGG-RNAP$_C$).

The Voigt group also discovered that RNA output in *E. coli* increased five to sevenfold over that of background assembly when positive interacting proteins were fused to each half of the RNAP. This foundational work inspired our group to evolve the split RNAP$_N$ to reassemble with any RNAP$_C$ *only* when interacting proteins are fused to each half (Fig. 2A). In brief, we used a new modified phage-assisted continuous evolution (PACE) system to evolve proximity-dependency in the split RNAP system, thereby making it into a biosensor platform. See the following reference for an in depth look at the evolution in *E. coli* and initial characterization of the evolved RNAP$_N$ (eRNAP$_N$) in both mammalian and *E. coli* cells, as well as our recent review that compares the split T7 RNAP biosensor to other PFC technologies (Jones, Kentala, et al., 2019; Jones, Zinkus-Boltz, et al., 2019; Pu, Zinkus-Boltz, & Dickinson, 2017).

2.2 eRNAP: Applications and advances

Overall, evolution of the split RNAP increased the signal-to-noise ratio from 5-fold to 300-fold over background in *E. coli*. The evolved split

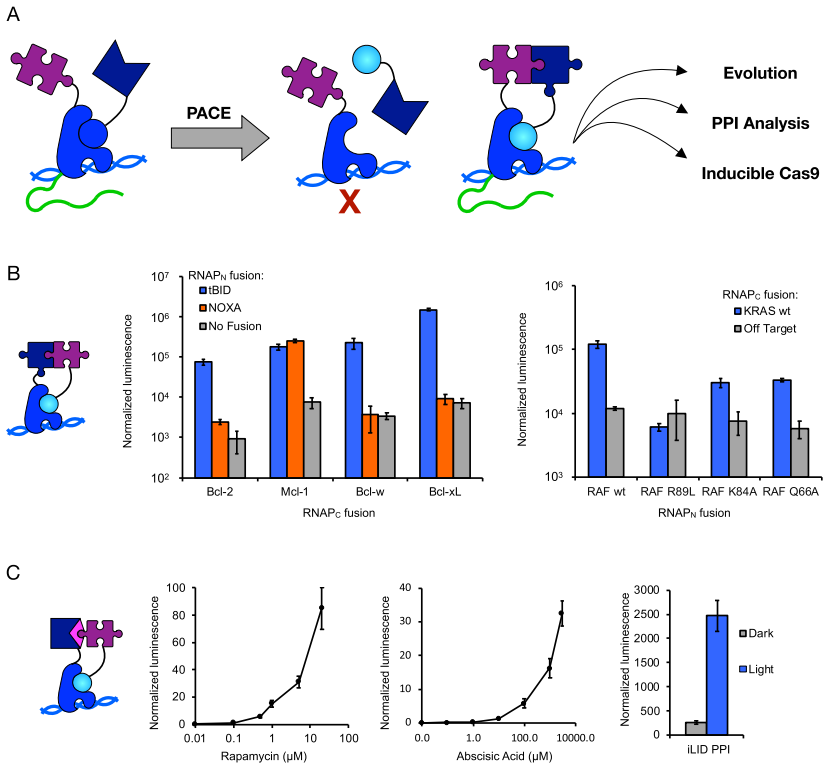

Fig. 2 Example interactions detected via the evolved split RNAP biosensor. (A) Representation of the split T7 RNAP's PPI detection properties prior to and after evolution of the $RNAP_N$. The wild type $RNAP_N$ will assemble even without interacting fusion proteins (left), whereas the evolved $RNAP_N$ only assembles when interacting proteins are fused to each fragment (middle). (B) *E. coli* luciferase assay results with Bcl-2 family (left) and KRas-Raf (right) interactions. (C) *E. coli* luciferase assay results with the small molecule and light inducible PPIs FRB-FKBP (left), PYL-ABI (middle), and iLID (right).

RNAP not only provided robust signal-to-noise (Fig. 2B), but also tolerated fusion to interacting proteins with diverse structures and activities including short helix proteins, globular proteins, and even activity-dependent PPIs that require small molecules or light to induce binding (Fig. 2C). We have recently used our evolved RNAP in two general ways: to study PPIs and for synthetic biology applications. For usage in evolution and small molecule-induced Cas9 gene circuits, see the following references (Pu, Disare, & Dickinson, 2019; Pu, Kentala, & Dickinson, 2018;

Pu, Zinkus-Boltz, et al., 2017. Recently, our group employed the RNAP biosensor to rapidly screen thousands of amino acid mutations across a PPI interface and assess their effects on protein binding (Zinkus-Boltz, DeValk, & Dickinson, 2019). In this work, we used Darwinian evolutionary principles combined with high throughput sequencing to perform a deep mutational scan of the Ras/Raf binding interface.

In this chapter we will focus on our work using the RNAP biosensor in live mammalian cells to monitor up to four PPIs simultaneously, and to interrogate pharmacological inhibition of the competitive PPI network (Pu, Dewey, Hadji, LaBelle, & Dickinson, 2017). Along with these major advances, this technology is still undergoing development and characterization, and so nuances regarding its mechanism, advantages, and disadvantages remain open to exploration. Notably, however, our group's recent and ongoing work has identified several key factors to consider when designing an experiment utilizing the evolved split RNAP.

2.3 Considerations when using the split RNAP

One major consideration whenever deploying the split RNAP biosensor is its access to a DNA template. In eukaryotic cells, DNA is separated from most proteins by lipid barriers that form the nucleus and other organelles. These physical barriers prevent the split RNAP from binding to its DNA promoter and subsequently transcribing an RNA signal. This is not usually a consideration when working with *E. coli* because they do not sequester DNA within compartments. Two notable exceptions are when investigating PPIs in the periplasm or extracellular space where DNA is inaccessible. Access to DNA is, however, a more pressing consideration when deploying this biosensor in mammalian cells, where many PPIs are localized within organelles that do not contain DNA, e.g., the Golgi or endoplasmic reticulum. Similarly, studying PPIs in the extracellular space and outer plasma membrane via the split RNAP is unlikely given that high concentrations of extracellular nucleotide triphosphates (NTPs), which are necessary to transcribe RNA, are toxic to cells (Agteresch, Dagnelie, van den Berg, & Wilson, 1999). The nucleus is therefore an optimal compartment for RNAP deployment because access to both DNA and NTPs is of minimal concern. Looking toward other compartments, manipulation of mitochondrial DNA to encode RNAP promoters, or DNA delivery techniques to endosomes/lysosomes in theory could enable PPI analysis via split RNAPs in these compartments (Chakraborty, Veetil, Jaffrey, & Krishnan, 2016).

A second major consideration when using the RNAP biosensor is the requirement for protein fusion. The RNAP tolerates different types of protein fusions, as our previous work has demonstrated. Yet, initially the $RNAP_C$ could not accept a C-terminal fusion because the wt $RNAP_C$ C-terminus is necessary for RNA transcription. In recent work, we overcame this disadvantage by evolving the $RNAP_C$ C-terminus to tolerate a protein fusion while retaining transcriptional capability (Pu et al., 2019). With this advance, both RNAP halves can now tolerate fusions to either termini, as long as the fusion proteins themselves drive reassembly of the RNAP. It is important to investigate whether a new PPI of interest, therefore, can properly orient the RNAP fragments. In our experience, there is a higher probability that protein fusions will be successful in the split T7 RNAP system if the proteins of interest have been previously used in other similar technologies, such as split GFP or split luciferase assays. If there is no precedent for protein fusion, then we find that crystal structure-based modeling or biochemical assays that reveal the roles of N- or C-termini in protein function, folding, and binding can greatly increase success when using the split T7 RNAP biosensor.

A third major consideration when deploying the split RNAP biosensor is the degradation, stability, folding, and overall activity of the fusion proteins. A relatively insoluble or unstable protein of interest fused to the RNAP fragments may result in differential expression of the resultant fusion protein, and in turn alter RNAP reassembly. As with all protein fusion approaches, the potential context-dependencies in protein stability or RNAP activity thus affect comparisons between PPIs. One PPI may produce a greater RNA signal simply due to improved RNAP folding/stability/activity rather than increased strength or frequency of the PPI in question. For this reason, it is crucial to run appropriate control experiments, particularly when comparing unique protein fusions to one another, or when assaying PPIs under different experimental conditions.

When designing experiments using the RNAP it is important to assess all of these factors and how they may change under each experiment's unique conditions. To ensure that results specifically reflect changes in PPIs of interest, and not changes in RNAP, the correct controls are critical. In the protocol below, we use our previous study of multiprotein interaction networks in live mammalian cells to describe the general workflow for designing a PPI detection experiment using proximity-dependent split RNAPs. Within this protocol we include troubleshooting tips and additional protocols for control experiments that are particularly useful when testing new protein fusions.

3. RNAP analysis of Bcl-2 family PPIs

Many PPIs exist within networks that operate via selective interactions. Most methods only study these PPIs individually. However, crosstalk between PPIs is important to understand and quantify, particularly in the case of pharmacology. Bcl-2 family proteins have been targeted by PPI inhibitors for cancer treatment, but resistance and off-target effects demand a holistic analysis of the Bcl-2 PPI network. Three protocols below detail experiments to study: (1) individual PPIs in *E. coli* using bacterial luciferase, (2) two PPIs simultaneously with small molecule inhibition by fluorescence microscopy, and (3) four PPIs simultaneously with small molecule inhibition via RNA quantification. For protocols on basic techniques such as cloning, *E. coli* transformation, mammalian cell transfection, etc., see references in Section 3.3.

3.1 Materials, equipment and reagents

LightCycler 96 qPCR (Roche)
Synergy Neo2 Hybrid Multi-Mode Plate Reader (BioTek)
BX53 fluorescence microscope (Olympus)
Sterile Gard biosafety cabinet (Baker)
Cell culture incubator 5% CO_2 (Thermofisher Scientific)
NanoDrop 8000 (Thermofisher Scientific)
HEK293T mammalian cells (ATCC)
DMEM with high glucose, L-glutamine, phenol red, sodium pyruvate (Gibco or Hyclone)
Fetal Bovine Serum (Gibco)
Penicillin/streptomycin (Gibco/Life Technologies)
Eight-well cover glass slides (Labtek)
Lipofectamine 3000 (Thermofisher Scientific)
ImageJ image processing software (Wayne Rasband, NIH)
12-Well plates (Corning)
RNeasy Kit (Qiagen)
PrimeScript TM RT reagent Kit (TaKaRa)
FastStart Essential DNA Green Master (Roche)
Opti-MEM I Reduced Serum Media (Thermofisher Scientific)
S1030 *E. coli* cells (Addgene)
96-Well black wall clear bottom plate (Nunc)
Plasmids and sequence maps can be found on addgene.org

3.2 Protocols

3.2.1 *Individual interactions in* E. coli

1. Transform 1030 *E. coli* cells (Carlson, Badran, Guggiana-Nilo, & Liu, 2014) with 2–22 reporter plasmid, 8–1 $RNAP_N$-tBID expression plasmid, and 7–79 BclxL-T7-$RNAP_C$ expression plasmid OR 2–39 ZB-T7-$RNAP_C$ expression plasmid (links to electronic maps found in Pu, Dewey, et al., 2017). General plasmid design found in Fig. 3A. Grow cells on agar plates containing all four antibiotics (tet, carb, chlor, spec) and glucose (to repress $RNAP_C$ expression) for 14–18 h at 37 °C.
2. Pick and grow four colonies of each plasmid combination in a 96 deep well plate until saturation (12–18 h) in 1 mL of LB (miller) media containing all four antibiotics and glucose.
3. Transfer 60 μL of each saturated culture to 540 μL of LB (miller) media in a 96 deep well plate containing all four antibiotics and arabinose (to activate $RNAP_C$ expression).

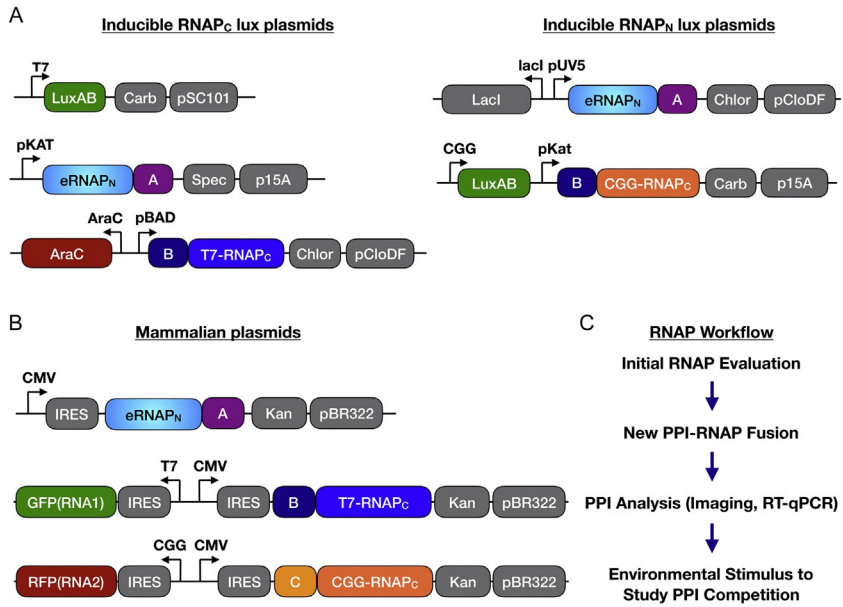

Fig. 3 Plasmid designs for *E. coli* and mammalian assays and general workflow when using the split RNAP biosensor. (A) Plasmid designs for measuring PPIs via bacterial luciferase in *E. coli* with arabinose induction of the $RNAP_C$ or IPTG induction of the $RNAP_N$. (B) Mammalian expression plasmid designs for use in imaging and RT-qPCR analyses. (C) General workflow when deploying RNAP biosensors to study proteins of interest. For more detailed assistance in designing experiments see Sections 3.2.1.1 and 3.2.2.1 of each protocol.

4. After 2 h (when cells are at ~0.2 optical density), and each hour thereafter, transfer 150 μL of culture to a clear bottom 96-well plate, and measure both absorbance at 600 nm to quantify *E. coli* optical density and luminescence output.
5. Analyze and normalize data using the following equation

$$\frac{lux_n - lux_0}{OD_n - OD_0}$$

Where lux_n is measured luminescence for a given sample, lux_0 is measured luminescence of LB media, OD_n is measured optical density for a given sample, and OD_0 is the optical density of LB media.

3.2.1.1 Troubleshooting and advice

Controls for split RNAP: *E. coli* lack many of the protein chaperones that mammalian cells rely on to properly fold newly-translated proteins. As a result, many mammalian proteins can be misfolded or aggregate in *E. coli*. If these misfolded proteins are fused to the RNAP they can interfere with, or completely eliminate, RNAP activity. Similarly, some proteins can cause the split RNAP to fold better, increasing its signal. The following control experiments are designed to test if a protein fusion changes RNAP activity.

3.2.1.1.1 Low signal

- Clone each protein of interest to the wild type $RNAP_N$.
- Transform *E. coli* with the new $wtRNAP_N$ fusion protein or a no fusion $wtRNAP_N$ control, a T7-$RNAP_C$ control (no fusion or ZB fusion), and T7 promoted luciferase.
- Perform luciferase assay as described above.
- If no signal is observed compared to the control wild type split RNAP assembly then the $RNAP_N$ activity is disrupted by the protein fusion.
- If $wtRNAP_N$ signal is observed, clone the proteins of interest as fusions to T7-$RNAP_C$ and repeat luciferase assay to assess if the protein of interest disrupts $RNAP_C$ activity.
- If signal is still observed with fusions to either RNAP half, but not when fused to test the proposed PPI itself, then the proteins do not interact with one another under these conditions.

3.2.1.1.2 High background

- To test if a high signal is dependent on the PPI of interest and not enhanced RNAP folding or expression, perform the same troubleshooting as with "low signal" above, but clone the proteins of interest as

fusions to the $eRNAP_N$. Also, use the interaction between $eRNAP_N$ without a fusion protein and $RNAP_C$ as the background activity.

- If signal is observed above the no fusion $eRNAP_N$ control interaction then the protein of interest most likely alters $RNAP_N$ stability or expression. Simply normalize the PPI of interest's activity to this higher background for more accurate analysis.

3.2.2 Imaging multiple interactions in mammalian cells

1. Culture HEK293T cells in triplicate for each PPI combination to 70–90% confluence in an eight-well cover glass slide dish with 250 μL antibiotic free DMEM media, supplemented with 10% fetal bovine serum and either 500 nM ABT-199 or DMSO control.
2. Transfect each well with 300 ng of 9–49 $RNAP_N$-tBID OR 9–52 $RNAP_N$-DeadBID mammalian expression plasmid, 300 ng of 9–54 T7 promoted GFP and BclxL-T7-$RNAP_C$ expression plasmid, 9–53 CGG promoted RFP and Mcl1-CGG-$RNAP_C$ expression plasmid, and 2.4 μL of lipofectamine 3000, while closely following the transfection protocol referenced in precursor techniques. See Fig. 3B for general mammalian plasmid designs.
3. After 24–36 h wash cells with 250 μL PBS incubate each well with 1 μM DAPI in PBS for at least 30 min to stain cell nuclei.
4. Within 2 h, using a fluorescence microscope with a 10 × objective, take white light, DAPI filtered (461 nm emission), GFP filtered (509 nm emission), and RFP filtered (583 nm emission) images of three random locations for each well.
5. Analyze GFP and RFP images using the following FIJI (Fiji is just image J) macro. For basic instructions on using ImageJ and designing ImageJ macros see precursor techniques below. "setThreshold" (X,4095); setOption ("BlackBackground," false); run ("Convert to Mask"); run ("Watershed"); run ("Analyze Particles…"), "size = Y − Infinity pixel include summarize in_situ." Where "X" is the threshold value at which 1% of total fluorescence remains for the average positive control sample, and where "Y" is the pixel size required to count a cell as "positive," which can affect results (Fig. 4B).
6. This script will provide the number of counted particles in a given image.

3.2.2.1 Troubleshooting and advice

3.2.2.1.1 DNA delivery Most cells of interest will not contain the T7 DNA promoter with a downstream reporter such as GFP or luciferase, so

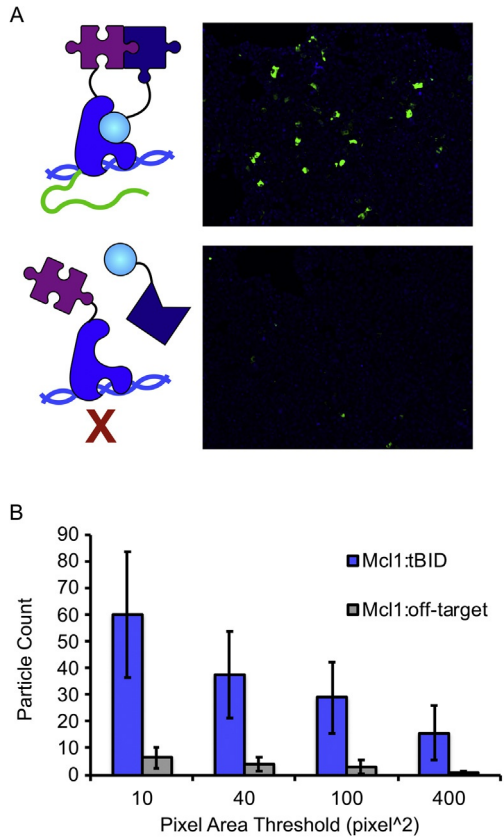

Fig. 4 Mcl1-tBID PPI detection in mammalian cells using a fluorescent RNA aptamer output. (A) Cells transfected with the $RNAP_N$ fused to either tBID (top image) or a truncated form of BID (bottom image), T7-$RNAP_C$ fused to Mcl1, and a T7 transcribed fluorescent RNA aptamer. An increased number of fluorescent cells was observed when positive interacting proteins were fused versus non-interacting proteins. (B) Graph demonstrating how analysis can vary based on pixel threshold values.

these sequences of DNA will need to be delivered by some method. Most of our work relies on transient transfection, which is outlined in Section 3.3. However, some cells are resistant to transient transfection. To determine if DNA can be delivered to your cells of interest, the transfection protocol above can be used with a DNA plasmid that constitutively expresses a reporter protein such as GFP, and then measure the percentage of reporter protein positive cells by microscopy.

3.2.2.1.2 Maximum split RNAP activity After successful DNA delivery, the RNAP activity itself should be assayed. Clone or purchase a

plasmid(s) with the following DNA elements: A T7 promoter-driven reporter protein (GFP, luciferase, etc.), constitutively expressed T7-$RNAP_C$, and constitutively expressed $wtRNAP_N$. Deliver the plasmid(s) and measure the signal via RT-qPCR, microscopy, or plate reader assay under your particular experimental conditions. To estimate a signal-to-noise ratio, conduct an experiment comparing reporter expression in the presence of $wtRNAP_N$, vs the $eRNAP_N$.

3.2.2.1.3 PPI fusion protein controls Perform the same control experiments as described above for the *E. coli* luciferase assay, instead using the appropriate plasmids for mammalian expression. First use fusions to the $wtRNAP_N$ to assess if protein fusion diminishes split RNAP activity. Next, use fusions to the $eRNAP_N$ to measure if protein fusion increases evolved split RNAP activity.

3.2.2.1.4 Multiple simultaneous PPI effects It is important to remember that the $RNAP_C$ contains the DNA promoter recognition domain and that mutations in this domain do not affect $RNAP_C$ assembly with $RNAP_N$. Therefore, all PPI experiments effectively involve one "hub" protein fused to the $RNAP_N$ and several potential binding partners fused to each orthogonal $RNAP_C$. For example, if, two $RNAP_N$ protein fusions, $RNAP_N$-A and $RNAP_N$-B, were introduced with a T7-$RNAP_C$ protein fusion into the same cells, it would be impossible to distinguish whether RNA signal was produced from $RNAP_N$-A, $RNAP_N$-B, or a combination of the two. Simply performing multiple experiments with different $RNAP_N$ protein fusions, and then normalizing the results to a control $RNAP_N$ or fusion protein can overcome this limitation.

One advantage of the split RNAP is its ability to measure competition between PPIs. For example, protein A might interact with both proteins B and C when tested individually, but when all three are expressed simultaneously or selectively inhibited, the A-B PPI may outcompete the A-C PPI (Fig. 5A). The split RNAP can take advantage of orthogonal $RNAP_C$ to encode a unique RNA signal for each PPI (Fig. 5B). However, any analysis of multiple simultaneous PPIs cannot assume the only difference between signals is due to PPI frequency. Along with considerations mentioned in Section 2.3, each orthogonal $RNAP_C$ and DNA promoter pair has a different activity and orthogonality profile. See Fig. 5A in the following reference for a large panel of $RNAP_C$ and DNA promoter pairs screened in *E. coli* (Pu, Dewey, et al., 2017). For example, the T7-$RNAP_C$ is able to recognize the K1F promoter to a significant degree. This means that decreasing

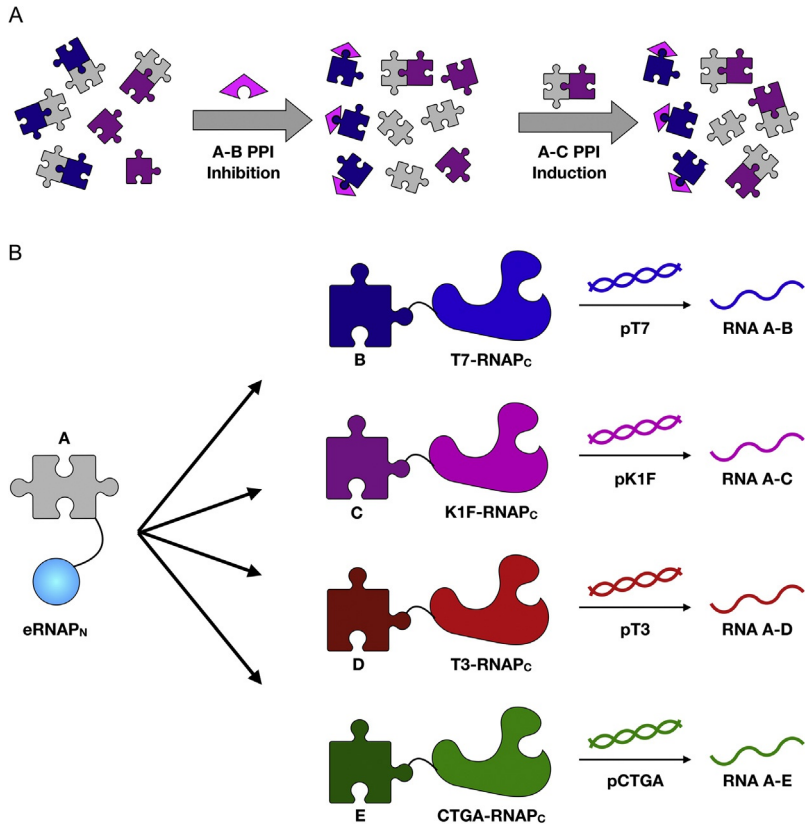

Fig. 5 PPI competition and multidimensional analysis using the split T7 RNAP biosensor. (A) Cartoon representing the importance of measuring multiple PPIs simultaneously in a given sample. Specifically, when a single PPI is inhibited (pink), it increases the unbound concentration of one binding partner (gray). The increased unbound protein concentration can increase its interactions with other proteins (purple), which may have different downstream impacts. (B) Cartoon portraying how the split RNAP biosensor can distinguish between at least four PPI simultaneously. In brief, the $RNAP_N$ can assemble with any of the mutant $RNAP_C$, but each $RNAP_C$ is orthogonal to one another. A protein fused to $RNAP_N$ will produce a different RNA signal depending on which $RNAP_C$ its protein partner is fused to. In this way, each PPI produces a unique RNA signal.

T7-$RNAP_C$ PPIs will also decrease K1F RNA signal, which could be mistaken for decreased K1F-$RNAP_C$ PPIs. There was no combination of $RNAP_C$ mutants and promoter pairs that would not have some mixed signal for a 1:4 (hub:potential partner) PPI based experiment. However, for a 1:3 PPI experiment, we would predict that using CTGA, K1F, and T3 promoters would have the fewest off-target effects, while for a 1:2 PPI

experiment, using the T7 and CGG promoters would have the fewest off-target effects (especially notable, since the original $RNAP_N$ evolution used these promoters).

3.2.2.1.5 Combining purified reagents and split RNAP tags

Combining split RNAP tags to study the perturbation or manipulation of PPIs by external triggers (like inhibitors) or endogenous signaling events presents an additional challenge: how to monitor PPIs over relatively short time periods. Split RNAP tags are empowered by the versatility of RNA. The signal can manifest in unique RNA sequences, RNA aptamers (e.g., spinach or broccoli) (Filonov, Moon, Svensen, & Jaffrey, 2014), or mRNA for reporter proteins such as GFP and luciferase. However, certain RNA signal outputs are more desirable in different situations. GFP and luciferase are commonly used due to reliability and cost effectiveness, but when monitoring signal changes within short time periods these slow folding and/or degradation of these proteins limit their use. When deploying split RNAP tags to monitor changes in PPIs on short time scales, which is common when using exogenous reagents, it's more effective to directly measure unique RNA sequences via either RT-qPCR or fluorescent RNA aptamers.

3.2.3 Monitoring a 4-by-1 PPI network during inhibitor treatment

1. Culture HEK293T cells in triplicate for each PPI combination to 70–90% confluence in 12-well culture plates with 250 μL antibiotic free DMEM media supplemented with 10% fetal bovine serum.
2. Transfect each well with 400 ng of 9–49 $RNAP_N$-tBID OR 9–52 $RNAP_N$-DeadBID mammalian expression plasmid, 400 ng of 9–54 T7 promoted GFP(RNA1) and Bcl2-T7-$RNAP_C$ expression plasmid, 10–52 T3 promoted RNA2 and Mcl1-T3-$RNAP_C$ expression plasmid, 11–63 CTGA promoted RNA3 and Bclw-CTGA-$RNAP_C$ expression plasmid, 12–75 K1F promoted RNA4 and BclxL-K1F-$RNAP_C$ expression plasmid and 6 μL of lipofectamine 3000, while closely following the transfection protocol referenced in precursor techniques.
3. Add 500 nM ABT-199 or DMSO control during transfection, 24 h after transfection, 36 h after transfection, and 45 h after transfection.
4. 48 h after transfection extract total RNA from cells using the RNAeasy kit from Qiagen. Note—when handling RNA be sure to use RNAse free reagents wipe down workbench with RNAse inhibitor.

5. Measure RNA concentration.
6. Perform reverse transcription. We recommend using PrimeScript TM RT kit. We didn't encounter issues when following the PrimeScript TM RT protocol.
7. Design qPCR primers for your RNA of interest and a housekeeping gene like GAPDH, or use those we used in the following reference (Pu, Dewey, et al., 2017).
8. Measure DNA concentration via qPCR. cDNA from reverse transcription was diluted 1:20 or 1:100 before adding to qPCR mixture. We found this necessary because the T7 RNAP biosensor produces large quantities of RNA in cells that saturate the qPCR signal. Save remaining DNA and rerun qPCR if CT values are less than 15 (implying too much cDNA) or above 32 (implying too little cDNA).
9. Subtract all Ct values by each sample's GAPDH Ct value to normalize RNA signal. This will ensure that samples with greater or fewer numbers of cells can still be compared to one another. Also, measuring the level of T7 RNA polymerase can help normalize for changes due to transfection.
10. Next, subtract from this GAPDH normalized value the average Ct value of an off-target control. For example, in this experiment we use a truncated form of tBID that no longer interacts with its binding partners. This provides a "ΔΔCt value" where the first Δ represents GAPDH normalization, and the second Δ represents off-target normalization.
11. To calculate RNA fold changes from Ct values simply use 2^{Ct}, so a ΔΔCt value of 4 would represent a 2^4 or 16 fold change in RNA between samples.

3.3 Precursor techniques

3.3.1 Cloning

Our group prefers cloning with the following techniques—electronic plasmid design, polymerase chain reaction (PCR), spin column DNA clean up, Gibson Assembly, and chemically competent *E. coli* transformation. Listed below are references for each technique.

Plasmid design—There are many electronic tools to aid in plasmid design. Our group uses the online services found on www.benchling.com. Benchling helps with many aspects of plasmid design including primer design, sequencing alignment, plasmid export, and Cas9 guide RNA design.

PCR—Our group amplifies sequences for later assembly using PCR. We purchase reagents from New England Biolabs (NEB), and follow their protocols. See the following website for a protocol using the high-fidelity Phusion DNA polymerase https://www.neb.com/protocols/0001/01/01/pcr-protocol-m0530.

DNA clean up—Although there are several ways to purify DNA, we purchase DNA spin/vacuum manifold columns from econospin, but use buffers and protocols found on Qiagen's website. Also, we use *Dpn*I treatment and/or gel purification to eliminate plasmid templates or alternative products from PCR reactions https://www.qiagen.com/us/resources/resourcedetail?id=e0fab087-ea52-4c16-b79f-c224bf760c39&lang=en.

Gibson Assembly—There are also many ways to assemble DNA into a plasmid. Our group uses a technique called Gibson Assembly. The following reference details this method and reagents needed (Gibson et al., 2009).

E. coli transformation—Our group uses protocols found in the following reference (Sambrook, Russell, & Sambrook, 2006).

3.3.2 Mammalian cell work

Transient transfection—See the following reference on mammalian cell transfection as a first look into this technique (Kim & Eberwine, 2010). We use lipofectamine 3000 or 2000, but polyethylenimine (PEI) can also be used. See the following references for Lipofectamine and PEI https://www.thermofisher.com/content/dam/LifeTech/global/life-sciences/CellCultureandTransfection/pdfs/Lipofectamine_3000_Protocol_6Dec2013.pdf (Longo, Kavran, Kim, & Leahy, 2013).

ImageJ—For help setting up a batch process see the following link https://imagej.net/Batch_Processing.

4. Summary

The split RNAP biosensor is a powerful tool to study multiple PPIs simultaneously in live cells. In particular, split RNAP tags are capable of studying changes in several PPIs over time depending on cellular environment and PPI competition. The most important consideration when deploying the split RNAP that isn't common to other protein fragment complementation assays is its requirement for a DNA template. Considering its limitations, we believe the split RNAP biosensor can spearhead a thorough PPI network analysis within cell nuclei, specifically when investigating PPI inhibition and competition. More critically, due to its

versatility and robust RNA output, the proximity-dependent split RNAP technology can be used for applications beyond just detection of PPIs, including synthetic biology applications to engineer gene circuits for cell control, selecting, and evolution.

Acknowledgments

This work was supported by the Yhim Foundation and the National Institute of General Medical Sciences (R35 GM119840) of the National Institutes of Health. J.D. was supported by a Multi-disciplinary Training program in Cancer Research from the National Institutes of Health (T32 CA009594).

References

Agteresch, H. J., Dagnelie, P. C., van den Berg, J. W., & Wilson, J. H. (1999). Adenosine triphosphate: Established and potential clinical applications. *Drugs*, *58*(2), 211–232. https://doi.org/10.2165/00003495-199958020-00002.

Carlson, J. C., Badran, A. H., Guggiana-Nilo, D. A., & Liu, D. R. (2014). Negative selection and stringency modulation in phage-assisted continuous evolution. *Nature Chemical Biology*, *10*(3), 216–222. https://doi.org/10.1038/nchembio.1453.

Chakraborty, K., Veetil, A. T., Jaffrey, S. R., & Krishnan, Y. (2016). Nucleic acid-based nanodevices in biological imaging. *Annual Review of Biochemistry*, *85*, 349–373. https://doi.org/10.1146/annurev-biochem-060815-014244.

Eliseev, B., Yeramala, L., Leitner, A., Karuppasamy, M., Raimondeau, E., Huard, K., et al. (2018). Structure of a human cap-dependent 48S translation pre-initiation complex. *Nucleic Acids Research*, *46*(5), 2678–2689. https://doi.org/10.1093/nar/gky054.

Filonov, G. S., Moon, J. D., Svensen, N., & Jaffrey, S. R. (2014). Broccoli: Rapid selection of an RNA mimic of green fluorescent protein by fluorescence-based selection and directed evolution. *Journal of the American Chemical Society*, *136*(46), 16299–16308. https://doi.org/10.1021/ja508478x.

Gibson, D. G., Young, L., Chuang, R. Y., Venter, J. C., Hutchison, C. A., 3rd, & Smith, H. O. (2009). Enzymatic assembly of DNA molecules up to several hundred kilobases. *Nature Methods*, *6*(5), 343–345. https://doi.org/10.1038/nmeth.1318.

Hall, M. P., Unch, J., Binkowski, B. F., Valley, M. P., Butler, B. L., Wood, M. G., et al. (2012). Engineered luciferase reporter from a deep sea shrimp utilizing a novel imidazopyrazinone substrate. *ACS Chemical Biology*, *7*(11), 1848–1857. https://doi.org/10.1021/cb3002478.

Hu, C. D., & Kerppola, T. K. (2003). Simultaneous visualization of multiple protein interactions in living cells using multicolor fluorescence complementation analysis. *Nature Biotechnology*, *21*(5), 539–545. https://doi.org/10.1038/nbt816.

Jones, K. A., Kentala, K., Beck, M. W., An, W., Lippert, A. R., Lewis, J. C., et al. (2019). Development of a split esterase for protein-protein interaction-dependent small-molecule activation. *ACS Central Science*, *5*(11), 1768–1776. https://doi.org/10.1021/acscentsci.9b00567.

Jones, K. A., Zinkus-Boltz, J., & Dickinson, B. C. (2019). Recent advances in developing and applying biosensors for synthetic biology. *Nano Futures*, *3*, 042002.

Kim, T. K., & Eberwine, J. H. (2010). Mammalian cell transfection: The present and the future. *Analytical and Bioanalytical Chemistry*, *397*(8), 3173–3178. https://doi.org/10.1007/s00216-010-3821-6.

Kim, S. J., Fernandez-Martinez, J., Nudelman, I., Shi, Y., Zhang, W., Raveh, B., et al. (2018). Integrative structure and functional anatomy of a nuclear pore complex. *Nature*, *555*(7697), 475–482. https://doi.org/10.1038/nature26003.

Langan, R. A., Boyken, S. E., Ng, A. H., Samson, J. A., Dods, G., Westbrook, A. M., et al. (2019). De novo design of bioactive protein switches. *Nature*, *572*(7768), 205–210. https://doi.org/10.1038/s41586-019-1432-8.

Longo, P. A., Kavran, J. M., Kim, M. S., & Leahy, D. J. (2013). Transient mammalian cell transfection with polyethylenimine (PEI). *Methods in Enzymology*, *529*, 227–240. https://doi.org/10.1016/B978-0-12-418687-3.00018-5.

Martell, J. D., Yamagata, M., Deerinck, T. J., Phan, S., Kwa, C. G., Ellisman, M. H., et al. (2016). A split horseradish peroxidase for the detection of intercellular protein-protein interactions and sensitive visualization of synapses. *Nature Biotechnology*, *34*(7), 774–780. https://doi.org/10.1038/nbt.3563.

Ozawa, T., Kaihara, A., Sato, M., Tachihara, K., & Umezawa, Y. (2001). Split luciferase as an optical probe for detecting protein-protein interactions in mammalian cells based on protein splicing. *Analytical Chemistry*, *73*(11), 2516–2521. https://doi.org/10.1021/ac0013296.

Plaschka, C., Hantsche, M., Dienemann, C., Burzinski, C., Plitzko, J., & Cramer, P. (2016). Transcription initiation complex structures elucidate DNA opening. *Nature*, *533*(7603), 353–358. https://doi.org/10.1038/nature17990.

Pu, J., Dewey, J. A., Hadji, A., LaBelle, J. L., & Dickinson, B. C. (2017). RNA polymerase tags to monitor multidimensional protein-protein interactions reveal pharmacological engagement of Bcl-2 proteins. *Journal of the American Chemical Society*, *139*(34), 11964–11972. https://doi.org/10.1021/jacs.7b06152.

Pu, J., Disare, M., & Dickinson, B. C. (2019). Evolution of C-terminal modification tolerance in full-length and split T7 RNA polymerase biosensors. *Chembiochem*, *20*(12), 1547–1553. https://doi.org/10.1002/cbic.201800707.

Pu, J., Kentala, K., & Dickinson, B. C. (2018). Multidimensional control of Cas9 by evolved RNA polymerase-based biosensors. *ACS Chemical Biology*, *13*(2), 431–437. https://doi.org/10.1021/acschembio.7b00532.

Pu, J., Zinkus-Boltz, J., & Dickinson, B. C. (2017). Evolution of a split RNA polymerase as a versatile biosensor platform. *Nature Chemical Biology*, *13*(4), 432–438. https://doi.org/10.1038/nchembio.2299.

Sambrook, J., Russell, D. W., & Sambrook, J. (2006). *The condensed protocols from molecular cloning: A laboratory manual*. Cold Spring Harbor, N.Y: Cold Spring Harbor Laboratory Press.

Segall-Shapiro, T. H., Meyer, A. J., Ellington, A. D., Sontag, E. D., & Voigt, C. A. (2014). A 'resource allocator' for transcription based on a highly fragmented T7 RNA polymerase. *Molecular Systems Biology*, *10*, 742. https://doi.org/10.15252/msb.20145299.

Shis, D. L., & Bennett, M. R. (2013). Library of synthetic transcriptional AND gates built with split T7 RNA polymerase mutants. *Proceedings of the National Academy of Sciences of the United States of America*, *110*(13), 5028–5033. https://doi.org/10.1073/pnas.1220157110.

Soucek, L., Whitfield, J. R., Sodir, N. M., Masso-Valles, D., Serrano, E., Karnezis, A. N., et al. (2013). Inhibition of Myc family proteins eradicates KRas-driven lung cancer in mice. *Genes & Development*, *27*(5), 504–513. https://doi.org/10.1101/gad.205542.112.

Souers, A. J., Leverson, J. D., Boghaert, E. R., Ackler, S. L., Catron, N. D., Chen, J., et al. (2013). ABT-199, a potent and selective BCL-2 inhibitor, achieves antitumor activity while sparing platelets. *Nature Medicine*, *19*(2), 202–208. https://doi.org/10.1038/nm.3048.

Stumpf, M. P., Thorne, T., de Silva, E., Stewart, R., An, H. J., Lappe, M., et al. (2008). Estimating the size of the human interactome. *Proceedings of the National Academy of Sciences of the United States of America*, *105*(19), 6959–6964. https://doi.org/10.1073/pnas.0708078105.

Sun, Y., Hays, N. M., Periasamy, A., Davidson, M. W., & Day, R. N. (2012). Monitoring protein interactions in living cells with fluorescence lifetime imaging microscopy. *Methods in Enzymology*, *504*, 371–391. https://doi.org/10.1016/B978-0-12-391857-4.00019-7.

Tabor, S., & Richardson, C. C. (1985). A bacteriophage T7 RNA polymerase/promoter system for controlled exclusive expression of specific genes. *Proceedings of the National Academy of Sciences of the United States of America*, *82*(4), 1074–1078. https://doi.org/10.1073/pnas.82.4.1074.

van der Geer, P. (2014). Analysis of protein-protein interactions by coimmunoprecipitation. *Methods in Enzymology*, *541*, 35–47. https://doi.org/10.1016/B978-0-12-420119-4.00004-5.

Wehr, M. C., & Rossner, M. J. (2016). Split protein biosensor assays in molecular pharmacological studies. *Drug Discovery Today*, *21*(3), 415–429. https://doi.org/10.1016/j.drudis.2015.11.004.

Zinkus-Boltz, J., DeValk, C., & Dickinson, B. C. (2019). A phage-assisted continuous selection approach for deep mutational scanning of protein-protein interactions. *ACS Chemical Biology*, *14*, 2757–2767. https://doi.org/10.1021/acschembio.9b00669.